Experimental study on the electrical properties of carbonaceous slate: A special natural rock with unusually high conductivity at high te....

Article *in* High Temperatures-High Pressures · November 2019

DOI: 10.32908/hthp.v48.749

CITATIONS
0

READS
142

6 authors, including:

Wenqing Sun
Institute of Geochemistry, Chinese Academy of Sciences
20 PUBLICATIONS **112** CITATIONS
SEE PROFILE

Lidong Dai
Chinese Academy of Sciences
88 PUBLICATIONS **950** CITATIONS
SEE PROFILE

Heping Li
Chinese Academy of Sciences
88 PUBLICATIONS **531** CITATIONS
SEE PROFILE

Haiying Hu
Chinese Academy of Sciences
50 PUBLICATIONS **434** CITATIONS
SEE PROFILE

High Temperatures-High Pressures, Vol. 48, pp. 439–454
Reprints available directly from the publisher
Photocopying permitted by license only
DOI: 10.32908/hthp.v48.749

Experimental study on the electrical properties of carbonaceous slate: a special natural rock with unusually high conductivity at high temperatures and pressures

Wenqing Sun[1,2], Lidong Dai[1,*], Heping Li[1], Haiying Hu[1], Jianjun Jiang[1] and Changcai Liu[1,2]

[1]*Key Laboratory of High-Temperature and High-Pressure Study of the Earth's Interior, Institute of Geochemistry, Chinese Academy of Sciences, Guiyang 550081, China*
[2]*University of Chinese Academy of Sciences, Beijing 100049, China*

Received: December 17, 2018; Accepted: February 7, 2019.

The electrical conductivities of carbonaceous slate were measured using a complex impedance spectroscopic technique at 0.5–1.5 GPa and 423–973 K in the frequency range of 10^{-1} to 3.5×10^{6} Hz. Experimental results indicate that the conductivities of carbonaceous slate slightly increased with increasing temperatures and pressures, respectively. At a certain temperature range, the conductivities of carbonaceous slate follow an Arrhenius relation. There are three Arrhenius relations for the conductivities of carbonaceous slate at a certain pressure. From high temperature range to low temperature range, the activation enthalpies for the conductivities of carbonaceous slate are found to be 0.02–0.03 eV, 0.05–0.06 eV, and 0.11–0.13 eV, respectively. Electron conduction is proposed to be the conduction mechanism for carbonaceous slate at high temperatures and pressures. It is suggested that the unusually high conductivities of carbonaceous slate (0.1–1 S/m) are associated to interconnected amorphous carbon. Furthermore, the electrical conductivities of carbonaceous rocks can be used to interpret the high-conductivity layers (HCLs) in the Earth's interior.

Keywords: Electrical conductivity, Carbonaceous slate, High pressure, Arrhenius relation, Conduction mechanism, High-conductivity layer

*Corresponding author: dailidong@vip.gyig.ac.cn

1 INTRODUCTION

Electrical conductivities of minerals, rocks, fluids and melts can be used to infer the material compositions and thermodynamic states in the Earth's interior. Previous studies have investigated the conductivities of most minerals and rocks in the Earth's crust and mantle [1–14], and the magnetotelluric (MT) and geomagnetic depth sounding (GDS) results have been provided significant constraints [1, 10, 15–17]. High conductivity layers are widely distributed in the middle-lower crust and upper mantle [18–21]. It has been confirmed that high conductivity anomalies can be caused by water in nominally anhydrous minerals [2–3, 22–23], dehydration of hydrous minerals [1, 10–11, 15–16, 24–27], interconnected saline (or aqueous) fluids [28–32], partial melting [33–41], interconnected secondary high conductivity phases [42–44] and graphite films on mineral grain boundaries [45–47]. In the subduction zones, the material compositions are very complicated, and high conductivity layers in these regions may be caused by various factors. As a special regional metamorphic rock, carbonaceous slate is widely distributed in subduction zones. However, the electrical conductivities of carbonaceous slate have not been investigated.

Previous studies have found that natural graphite was formed in regional metamorphic rocks (e.g., gneiss, granulite and metapelite), and the maximum content of graphite is about 25 vol% [48–51]. There are four formation mechanisms for natural graphite: metamorphism of biogenetic carbonaceous material; migration of mantle-derived graphite; sedimentation of carbonaceous aqueous fluids; reduction reaction of carbonates [49, 52]. The graphite in metamorphic rocks may be formed by the metamorphism of amorphous carbon in carbonaceous slate at high temperatures and pressures. In the process of subduction, carbonaceous slate is gradually changed into schist, gneiss and granulite, and graphite is formed at high temperatures and pressures [48, 51]. Furthermore, diamond is widely distributed in ultrahigh pressure metamorphic rocks (UHPM) [53, 54], and the diamond may be closely related to carbonaceous material from the shallow crust. Therefore, the carbonaceous rocks entering into the Earth's interior may play very important roles on the carbon cycle, electrical behavior, and redox conditions in the subduction zones. It is significant to research the electrical conductivity of carbonaceous slate at high temperatures and pressures.

In the present study, we in-situ measured the electrical conductivity of the carbonaceous slate samples under the conditions of 0.5–1.5 GPa and 423–973 K. The effect of temperature and pressure on the conductivity of carbonaceous slate was researched in detail. According to the calculated activation enthalpies and the results of previous studies, we also explored the conduction mechanisms for the carbonaceous slate. Finally, the electrical conductivities of carbonaceous slate were compared with those of other relevant minerals and rocks.

2 EXPERIMENTAL PROCEDURES

2.1 Sample preparation

The carbonaceous slate sample was collected from the metamorphic terrain in chongan, Zhejiang, China. The surface of experimental sample was fresh, non-oxidized and non-fractured. In order to determine the mineralogical assemblage of the sample, we applied the optical microscopy, scanning electron microscope (SEM) and X-ray diffraction (XRD) at the State Key Laboratory of Ore Deposit Geochemistry, Institute of Geochemistry, Chinese Academy of Sciences (CAS), Guiyang, China. According to the characters under the optical microscopy, quartz, chlorite and muscovite in the carbonaceous slate were observed (Fig. 1). However, the black minerals can not be determined using the optical microscopy. Based on the component analysis of scanning electron microscope-energy dispersive X-ray (SEM-EDX), carbon was confirmed to be the main element of the black minerals (Fig. 2). Meanwhile, there was no characteristic peak of graphite in the XRD spectra of carbonaceous slate (Fig. 3). Therefore, it was determined that the black minerals were amorphous carbon distributed in the surface of quartz. As shown in Fig. 1 and Table 1, the main minerals of carbonaceous slate are quartz, amorphous carbon and chlorite, and muscovite is the accessory mineral of the carbonaceous slate.

The carbonaceous slates were ground (<200 mesh) to ensure the homogeneous distribution of minerals. In order to remove the absorbed water, the powder was dried at 473 K for 6 h in a muffle furnace. Then the powder was

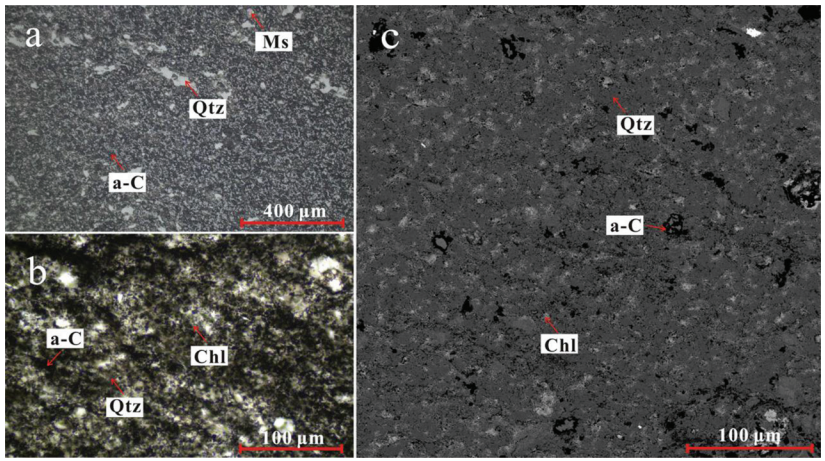

FIGURE 1
Photomicrographs of carbonaceous slate (a) in reflected light mode, (b) in transmitted light mode, and (c) electron backscattered images. Qtz represents quartz, Chl represents chlorite, a–c represents amorphous carbon and Ms represents muscovite.

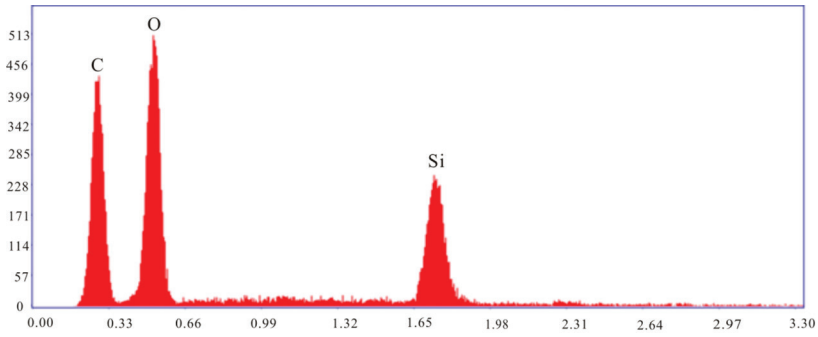

FIGURE 2
The scanning electron microscope-energy dispersive X-ray (SEM-EDX) spectra of black minerals in the carbonaceous slate.

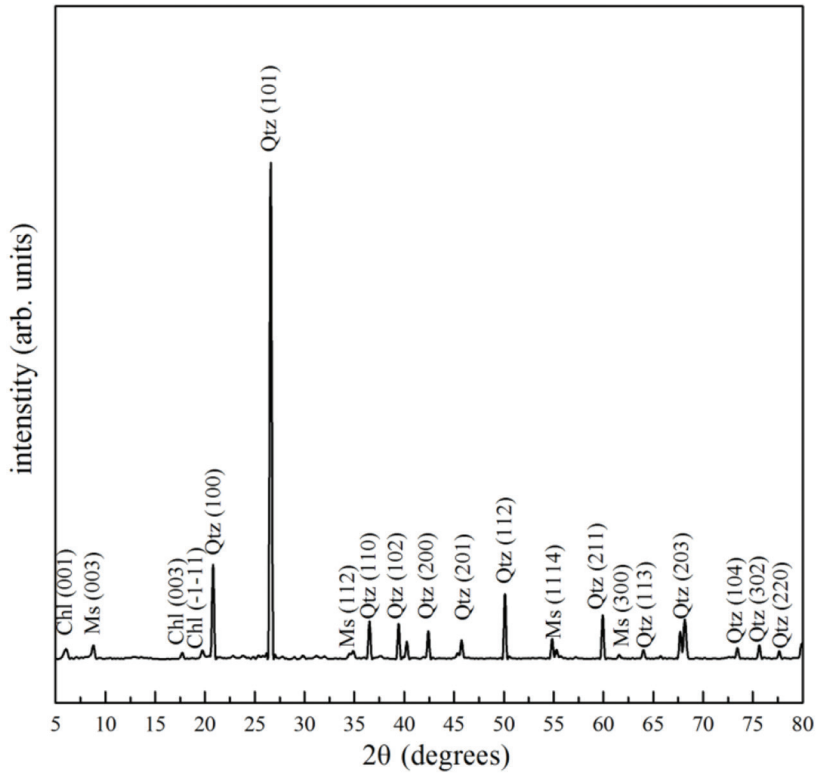

FIGURE 3
X-ray diffraction (XRD) patterns of carbonaceous slate. Qtz represents quartz, Chl represents chlorite, and Ms represents muscovite.

TABLE 1
Fitted parameters of the Arrhenius relation for the electrical conductivities of the carbonaceous slate sample.

Run No.	P (GPa)	T (K)	Log σ_0 (S/m)	ΔH (eV)	R^2
		423–523	−0.53±0.01	0.02±0.01	0.9994
DS15	0.5	573–773	−0.31±0.01	0.05±0.01	0.9956
		823–973	0.04±0.01	0.11±0.01	0.9999
		423–523	−0.47±0.01	0.02±0.01	0.9993
DS16	1.0	573–773	−0.12±0.01	0.06±0.01	0.9972
		823–973	0.31±0.01	0.13±0.02	0.9986
		423–523	−0.09±0.02	0.03±0.01	0.9938
DS17	1.5	573–773	0.17±0.02	0.06±0.01	0.9928
		823–973	0.57±0.06	0.12±0.02	0.9938

loaded into a copper capsule with a 0.025 mm thick nickel (Ni) foil liner, and the powdered carbonaceous slate sample was hot-pressed for 4 h in a multi-anvil high-pressure apparatus at 1.5 GPa and 673 K. The hydrothermally annealed samples were cut and polished into cylinders with diameters and heights of 6 mm, and then cleaned in an ultrasonic cleaning device using the mixed liquid of deionized water, acetone and ethanol. Furthermore, the cylindrical samples were heated at 473 K for 8 h in an oven to eliminate absorbed water for subsequent measurements.

2.2 Impedance measurements

The in situ measurements of electrical conductivity were performed using a YJ-3000t multi-anvil apparatus and the Solartron-1260 Impedance/Gain-phase analyzer at the Key Laboratory of High-Temperature and High-Pressure Study of the Earth's Interior, Institute of Geochemistry, Chinese Academy of Sciences, Guiyang, China. The multi-anvil press and Solartron-1260 Impedance/Gain-phase analyzer have been widely applied to research the electrical conductivities of natural minerals and rocks (e.g., olivine, feldspar, granite, gneiss, pelites) [2–11, 24–25]. For the multi-anvil press, six cubic WC anvils were assembled and compressed to generate hydrostatic pressure (Fig. 4), and the pressures in the sample capsule are up to 6.0 GPa. Generally, temperatures of up to 1573 K can be achieved using a stainless steel heater. The errors of experimental temperatures and pressures are ±5 K and ±0.1 GPa, respectively. The experimental assemblage for electrical conductivity measurements on carbonaceous slate is shown in Fig. 5. In advance, all components of sample assembly (pyrophyllite, ceramic tubes, Al_2O_3 and MgO sleeves) were baked at 1073 K in a muffle furnace for 8 hrs. In the sample assembly, the sample was loaded into the magnesia tube, and

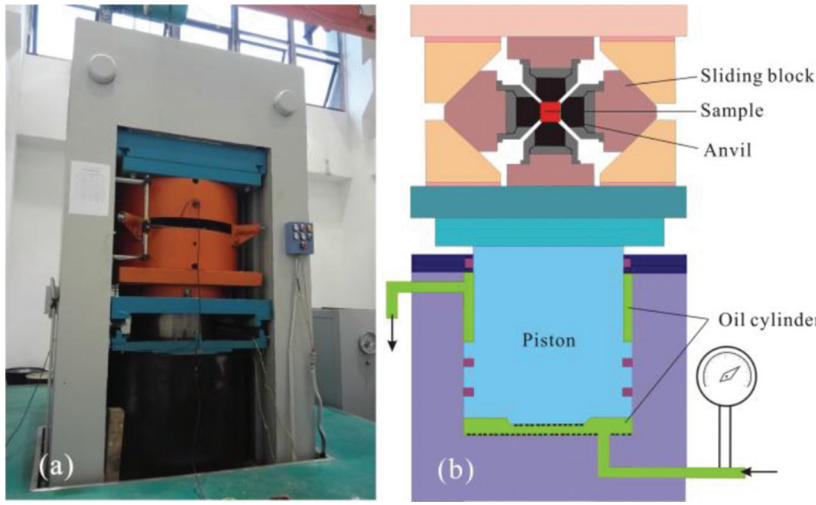

FIGURE 4
The image (a) and internal structure diagram (b) of the YJ-3000t multi-anvil apparatus.

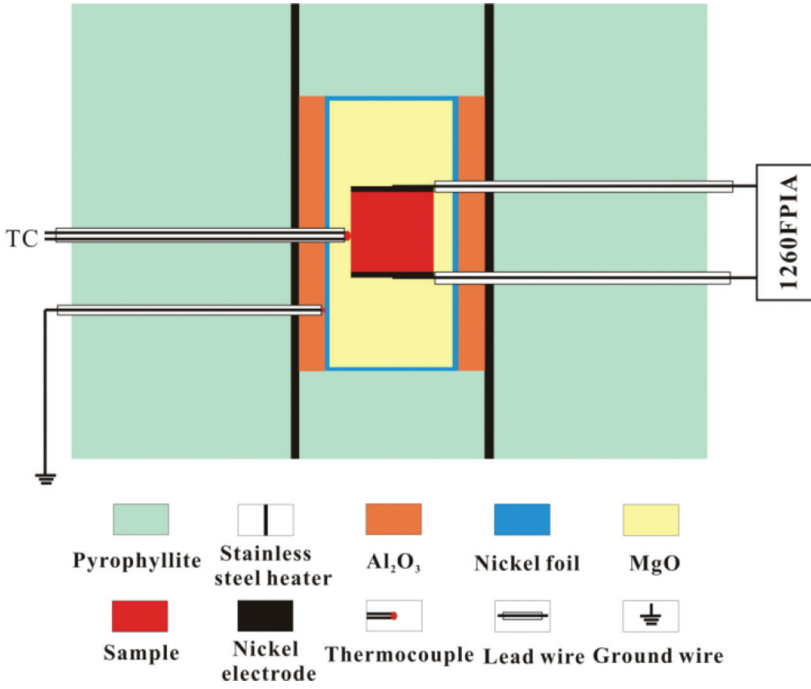

FIGURE 5
Sample assembly for electrical conductivity measurements at high temperatures and pressures.

two nickel disks on the top and bottom of the sample were applied to be the electrodes (diameter: 6.0 mm and thickness: 0.5 mm). In order to shield against the external electromagnetic and spurious signal interference, a layer of nickel foil with the thickness of 0.025 mm was installed between the alumina and magnesia sleeve. Alumina and magnesia sleeves between heater and sample have good properties of insulating and transmitting pressure. The three-layer stainless steel sheets (total thicknes: 0.5 mm) and pyrophyllite cube (32.5 × 32.5 × 32.5 mm^3) were applied to be heater and pressure medium, respectively. Before conducting electrical conductivity measurements, the sample assembly was placed in an oven at 323 K to avoid the effect of moisture.

During the experiments, pressure was slowly raised at a rate of 1.0 GPa/h until it reached the desired value, and then the temperature was increased at the rate of 600 K/h to the designated values. The impedance spectra of samples with an applied voltage of 1 V and the frequency range of 10^{-1}–3.5×10^{6} Hz were collected when desired pressure and temperature were stable. At the desired pressure, the spectra were measured at a certain temperature which was changed in 50 K intervals. In order to demonstrate the reproducibility of data, the electrical conductivities of the sample were measured in two heating and cooling cycles at the pressure of 0.5 GPa and 423–973 K. In the entire measurement process, the impedance spectra of carbonaceous slate sample were collected under the conditions of 0.5–1.5 GPa and 423–973 K.

3 RESULTS

Representative complex impedance spectra of the carbonaceous slate sample at 0.5 GPa and 423–973 K are displayed in Fig. 6. The impedance spectra are composed of an almost ideal semicircle in the high-frequency domain and an additional tail in the lower frequency domain. The impedance spectra of the carbonaceous slate are similar to those of hydrous olivine [55] and the dehydration product of epidote [10]. In general, the ideal semicircle of rocks at high frequencies represents the impedance of the grain interior, and the other part at low frequencies reflects the characteristic of diffusion processes at the sample-electrode interface [10, 55–57]. For the impedance spectra of carbonaceous slate, the additional tail with positive Z'' may reflect the effect of inductive impedance. Therefore, the resistance of carbonaceous slate can be obtained by fitting the ideal semicircle at high frequencies. A parallel connection of R_S-CPE_S (R_S and CPE_S represent the resistance and constant-phase element of the sample, respectively) was applied to be the equivalent circuit [10, 14], and the fitting errors of the electrical resistance were less than 5 %. The electrical conductivity of the sample was calculated by the following formula:

$$\sigma = L / SR, \tag{1}$$

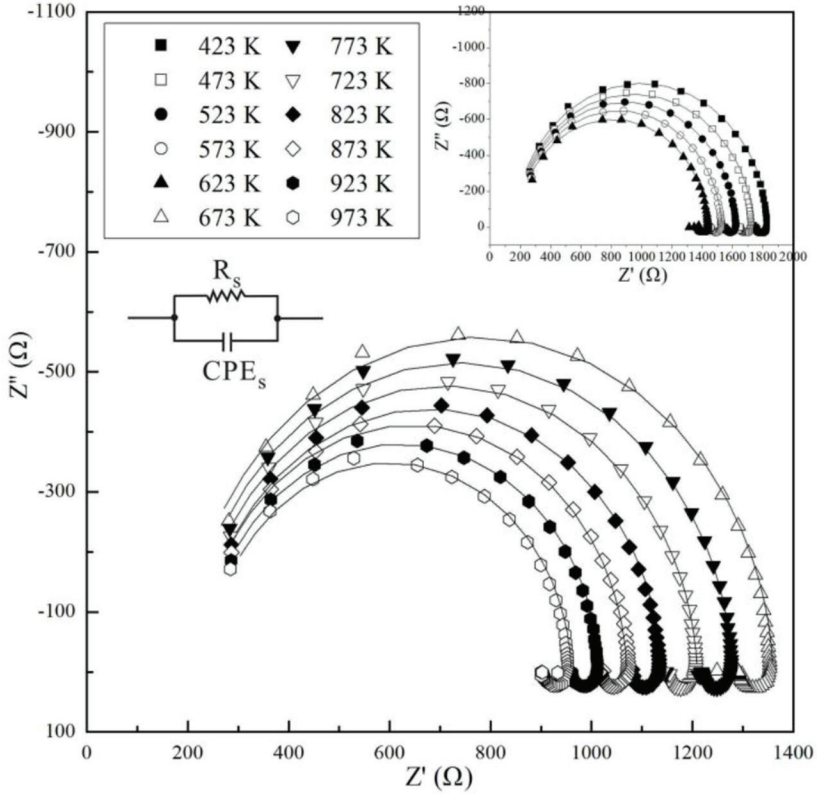

FIGURE 6
Nyquist plot of the complex impedance of carbonaceous slate at 0.5 GPa and 423–973 K.

where L is the height of the sample (m), S is the cross-sectional area of the electrodes (m^2), R is the fitting resistance (Ω) and σ is the electrical conductivity of the sample (S/m).

Under the conditions of 0.5 GPa and 423–973 K, the relationship between electrical conductivities of the carbonaceous slate and temperatures in three heating/cooling cycles are shown in Fig. 7. The conductivity of carbonaceous slate in the previous two heating/cooling cycles gradually increased at the same temperature, but remained stable in the third heating/cooling cycle. It was indicated that the sample has been stable after two heating/cooling cycles. The logarithmic electrical conductivities of the carbonaceous slate were plotted against the reciprocal temperatures under the conditions of 0.5–1.5 GPa and 423–973 K (Fig. 8). At a certain pressure, the conductivity of carbonaceous slate slightly increased with the increase of temperature. In addition, the conductivity of the sample weakly decreased with increasing pressure. As shown in Fig. 8, there are three linear relations of logarithmic

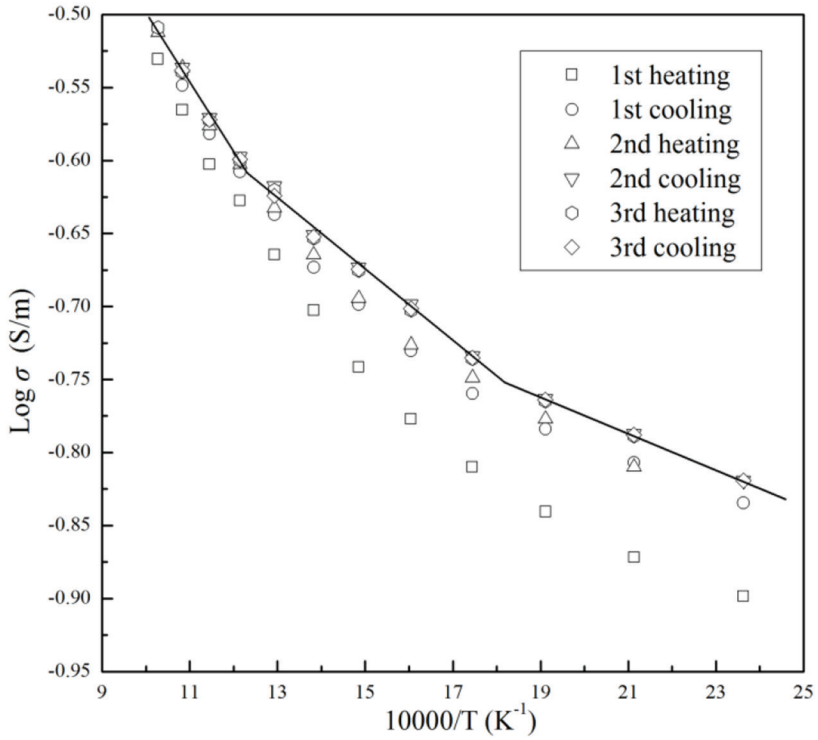

FIGURE 7
Logarithm of electrical conductivities versus reciprocal temperatures for the carbonaceous slate during 3 heating/cooling cycles at 0.5 GPa and 423–973 K.

electrical conductivity and reciprocal temperature, and thus the electrical conductivities of the carbonaceous slate and temperatures conform to an Arrhenius relation in a certain temperature region. The slopes of three linear regions slightly increased from low temperature region to high temperature region. The Arrhenius formula of electrical conductivity of carbonaceous slate and temperature is shown as follows:

$$\sigma = \sigma_0 \exp(-\Delta H / kT), \tag{2}$$

where σ_0 is the pre-exponential factor (K·S/m), k is the Boltzmann constant (eV/K), T is the absolute temperature (K), and ΔH is the activation enthalpy (eV). The relevant fitting parameters for the electrical conductivities of carbonaceous slate are listed in Table 1. The pre-exponential factor gradually increased from low temperature region to high temperature region, and the activation enthalpies were 0.02–0.13 eV under the experimental conditions.

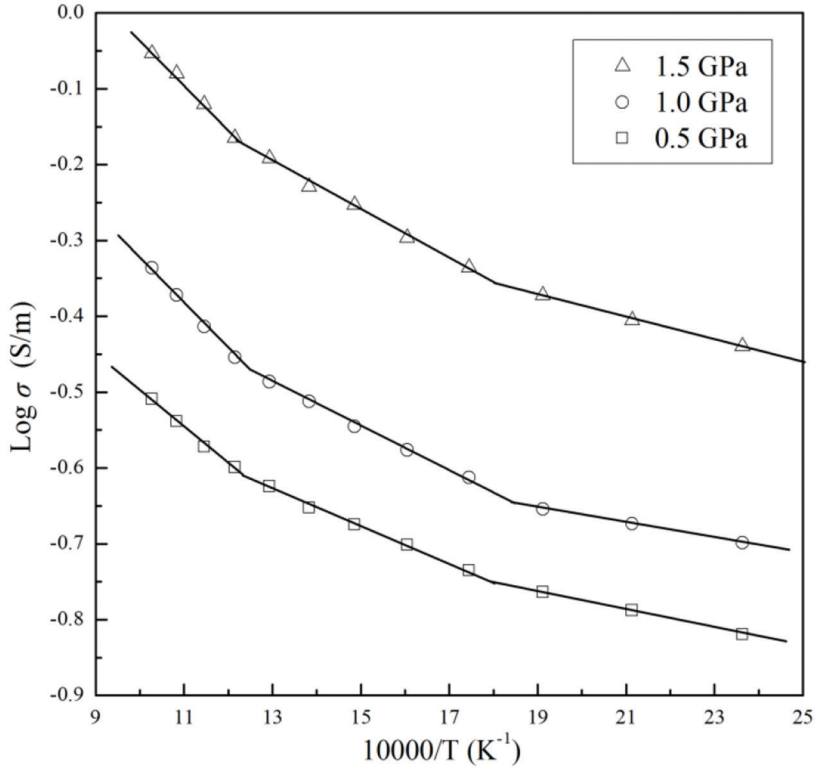

FIGURE 8
Relationship between logarithmic electrical conductivities of carbonaceous slate and reciprocal temperatures at 0.5–1.5 GPa and 423–973 K.

4 DISCUSSION

4.1 Conduction mechanism

The logarithmic electrical conductivities and reciprocal temperatures conform to three different linear relations from the low temperature region to the high temperature region. Activation enthalpy is a crucial parameter to determine the charge carriers in various minerals and rocks [10, 24–25, 58–60]. In order to investigate the conduction mechanism for carbonaceous slate, we fitted the thermodynamic parameters for electrical conductivities of the carbonaceous slate. As shown in Table 1, the activation enthalpies for the electrical conductivities of carbonaceous slate are 0.02–0.13 eV. At high temperatures and pressures, the conduction mechanisms for most minerals and rocks are electron conduction, small polaron conduction, ionic conduction, proton conduction or impurity conduction [5, 7, 10, 12, 58–60]. The activation enthalpies of ionic conduction for silicate minerals and rocks (>2 eV)

are very high due to the difficulty in the formation and migration of cation vacancies at high pressures [9]. Furthermore, the activation enthalpies for silicate minerals and rocks with hydrogen conduction and small polaron conduction are higher than 0.6 eV [10, 16, 25]. For minerals and rocks with impurity conduction, the activation enthalpies of electrical conductivities are about 0.5–1.2 eV [5, 61]. The activation enthalpies for carbonaceous slate were much lower than those for minerals and rocks with the conduction mechanisms of hydrogen conduction, small polaron conduction, ionic conduction and impurity conduction. Previous study has researched the electrical conductivities and conduction mechanism of olivine aggregates with 7 vol% graphite at high temperatures and pressures [58]. The activation enthalpies for olivine aggregates with interconnected graphite (0.04–0.17 eV) are much lower than those for pure olivine aggregates (1.28 eV) [4, 58]. Apparently, it was caused by the interconnected graphite on the boundary of olivine grain. The activation enthalpies for carbonaceous slate (0.02–0.13 eV) are very close to the values for olivine aggregates with 7 vol% graphite (0.04–0.17 eV) [58]. Therefore, we propose that electron conduction is the conduction mechanism for carbonaceous slate at high temperatures and pressures, and the slight difference of the activation enthalpies for carbonaceous slate at various temperature regions may be caused by the various structures of amorphous carbon.

4.2 Comparisons with previous studies

The main minerals of the natural carbonaceous slate sample are quartz, chlorite, and amorphous carbon, and each mineral has a good interconnectivity. Therefore, the electrical conductivity of carbonaceous slate is dominated by the mineral with the highest conductivity. The mineralogical assemblage and structure of most rocks are very complicated, so the chemical and physical changes of the rocks always occur at high temperatures and pressures. It's always needed enough time to make experimental sample reach steady state. As shown in Fig. 7, the electrical conductivities of carbonaceous slate in the first heating/cooling cycles and the second heating cycle are slightly lower than those in the second cooling cycle and the third heating/cooling cycles. This indicates that the carbonaceous slates are unstable in the first heating/cooling cycles and the second heating cycle. In the multiple heating/cooling cycles, the change rule of the electrical conductivities of carbonaceous slate is similar to those of other silicate rocks (e.g., gneiss, granulite, metasedimentary rock, eclogite, granite and basalt), and metamorphic effect of the rocks did not occur under the experimental conditions [5–6, 34, 62–63]. This implies that the structure and distribution of chemical compositions of most silicate rocks are slightly altered at high temperatures and pressures. Previous study has found that graphite in granulite is formed at the temperatures over 973 K [64]. The dehydration temperature of phlogopite is over 1273 K at 1.0 GPa, and the dehydration temperatures of chlorite is about

1023 K at 1.5 GPa. In addition, the relationship between electrical conductivities of carbonaceous slate and temperatures in the first heating cycle is consistent with those in other heating/cooling cycles (Fig. 7). Therefore, the metamorphism of carbonaceous slate didn't occur at the present experimental conditions.

Under the conditions of 0.5–1.5 GPa, the electrical conductivities of carbonaceous slate were increased by 0.3 orders of magnitude from 423 K to 973 K. This indicates that the influence of temperature on the conductivities of carbonaceous slate is weak, and the phenomenon is different from that for most silicate minerals and rocks [2–6, 65]. In addition, the electrical conductivities of carbonaceous slate increased with increasing pressure, and the conductivities of the slate sample was increased by 0.4 orders of magnitude from 0.5 GPa to 1.5 GPa at a certain temperature. The weak effect of pressure on the conductivities of carbonaceous slate was similar to that of most silicate rocks [5–7]. The previous study has investigated the electrical conductivity of synthetic quartz at 850–1600 K and 1.0 GPa [61]. The conductivities of quartz are much lower than those of carbonaceous slate at high temperatures and pressures. The conductivities of chlorite are also much lower than the values of carbonaceous slate. Furthermore, the slopes of the linear relation between the logarithmic electrical conductivity of chlorite and the reciprocal temperature are much higher than the slopes for the carbonaceous slate samples [16]. Therefore, the electrical conductivity of carbonaceous slate is not dominated by quartz or chlorite, and amorphous carbon is the most conductive material in carbonaceous slate. Electrical conductivities of olivine aggregates with 7 vol% graphite were two orders of magnitude higher than those of carbonaceous slate at high temperatures and pressures (Fig. 9) [58]. This indicates that electrical conductivity of amorphous carbon is lower than that of graphite. Micas are important hydrous minerals in the subduction zones, so it is necessary to compare the electrical conductivities of carbonaceous slate with those of micas. As shown in Fig. 9, the electrical conductivities of carbonaceous slate are much higher than those of phlogopite and phengite at temperatures of 423–973 K. In addition, the electrical conductivities of gneiss samples with $W_A = 14.79$ wt% are much lower than those of carbonaceous slate. Granulite is another significant metamorphic rock which is widely distributed in regional metamorphic belts. It's important to compare the conductivities of carbonaceous slate with the values of granulite. The conductivities of carbonaceous slate are two orders of magnitude higher than the value of granulite at high temperatures and pressures [62]. Furthermore, the electrical conductivities of pelites before and after dehydration are lower than those of carbonaceous slate [24, 25]. Finally, the unusually high conductivities of carbonaceous slate (0.1–1 S/m) were close to those of high conductivity layers in the middle–lower crust and upper mantle (0.01–1 S/m) [66–69]. Therefore, the presence of carbonaceous rocks can be used to interpret the high conductivity anomalies in the Earth's interior.

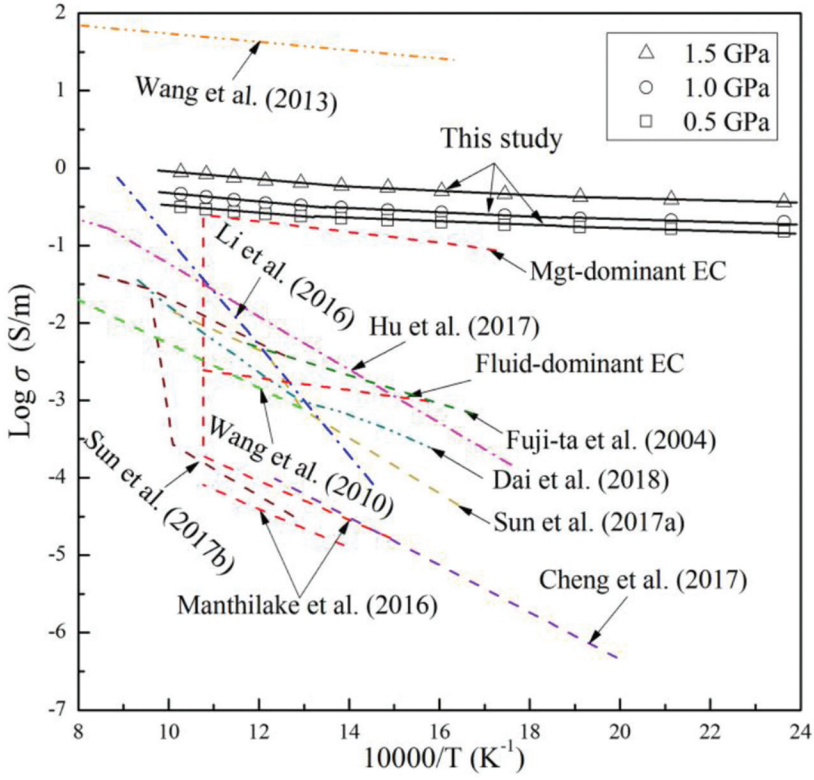

FIGURE 9
Comparison of the electrical conductivities of carbonaceous slate and the results of previous studies. The dashed green line represents the electrical conductivities of granulite at 1.0 GPa [62], the dashed light green represents the electrical conductivity of quartz at 1.0 GPa [61], the dashed wheat lines represent the electrical conductivity of olivine aggregates with 7 Vol% graphite at 4.0 GPa [58], the dashed blue line represents the electrical conductivity of phlogopite at 1.0 GPa [12], the dashed red line represents the electrical conductivity of chlorite at 2.0 GPa and 4.0 GPa [16], the dashed brown line represents the electrical conductivity of mudstone at 1.5 GPa [24], the dashed dark red line represents the electrical conductivity of phyllite at 1.5 GPa [25], the dashed pink line represents the electrical conductivity of epidote at 1.5 GPa [10], the dashed purple line represents the electrical conductivity of phengite at 2.3 GPa [1], and the dashed powder blue line represents the electrical conductivity of gneiss at 1.5 GPa [7].

5 CONCLUSIONS

The electrical conductivities of carbonaceous slate slightly increased with the increase of temperature and pressure, respectively. The influence of temperature on the conductivities of carbonaceous slate was much weaker than that of most silicate rocks. Under the conditions of 0.5–1.5 GPa and 423–973 K, the conductivities of carbonaceous slate were 0.1–1 S/m. Our findings indicate that carbonaceous slate is a natural rock with unusually high electrical

conductivity at high temperatures and pressures. The unusually high electrical conductivity of carbonaceous slate (0.1−1 S/m) is proposed to be caused by interconnected amorphous carbon. At a certain temperature range, the conductivities of carbonaceous slate and temperatures conform to an Arrhenius relation, and the fitted activation enthalpies are 0.02–0.13 eV. Electron conduction is proposed to be the conduction mechanism for carbonaceous slate. Furthermore, the slight difference of the activation enthalpies for carbonaceous slate at various temperature regions may be caused by the different structures of amorphous carbon. Finally, the electrical conductivities of carbonaceous slate are close to those of highly conductive layers in the middle-lower crust and upper mantle. Therefore, carbonaceous rocks might be a significant influence factor on the high conductivity anomalies in the Earth's interior.

ACKNOWLEDGEMENTS

This research was financially supported by the Strategic Priority Research Program (B) of the Chinese Academy of Sciences (XDB 18010401), Key Research Program of Frontier Sciences of CAS (QYZDB-SSW-DQC009), "135" Program of the Institute of Geochemistry of CAS, Hundred Talents Program of CAS and NSF of China (41474078, 41774099 and 41772042).

REFERENCES

[1] Chen, S. B., Guo, X. Z., Yoshino, T., Jin, Z. M., Li, P. *Geology*, 46(2018), 11–14, https://doi.org/10.1130/G39716.1
[2] Dai, L. D., Karato, S. I. *Earth Planet. Sc. Lett.*, 287(2009), 277–283, https://doi.org/10.1016/j.epsl.2009.08.012
[3] Dai, L. D., Karato, S. I. Phys. *Earth Planet. Inter.*, 237(2014), 73−79, https://doi.org/10.1016/j.pepi.2014.10.006
[4] Dai, L. D., Li, H. P., Hu, H. Y., Shan, S. M. *J. Geophys. Res. Solid Earth*, 113(2008), B12211, https://doi.org/10.1029/2008JB005820
[5] Dai, L. D., Hu, H. Y., Li, H. P., Jiang, J. J., Hui, K. S. *Am. Mineral.*, 99(2014), 1420−1428, https://doi.org/10.2138/am.2014.4692
[6] Dai, L. D., Hu, H. Y., Li, H. P., Wu, L., Hui, K. S., Jiang, J. J., et al. *Geochem. Geophys. Geosyst.*, 17(2016), 2394–2407, https://doi.org/10.1002/2016GC006282
[7] Dai, L. D., Sun, W. Q., Li, H. P., Hu, H. Y., Wu, L., Jiang, J. J. Solid Earth, 9(2018), 233−245, https://doi.org/10.5194/se-9-233-2018
[8] Hu, H. Y., Li, H. P., Dai, L. D., Shan, S. M., Zhu, C. M. Phys. Chem. Miner., 40(2013), 51−62, https://doi.org/10.1007/s00269-012-0546-4
[9] Hu, H. Y., Dai, L. D., Li, H. P., Jiang, J. J., Hui, K. S. Miner. Petrol., 108(2014), 609–618, https://doi.org/10.1007/s00710-014-0325-7
[10] Hu, H. Y., Dai, L. D., Li, H. P., Hui, K. S., Sun, W. Q. J. Geophys. Res. Solid Earth, 122(2017), 2751−2762, https://doi.org/10.1002/2016JB013767
[11] Hu, H. Y., Dai, L. D., Li, H. P., Sun, W. Q., Li, B. S. Earth Planet. Sc. Lett., 498(2018), 27−37, https://doi.org/10.1016/j.epsl.2018.06.003
[12] Li, Y., Yang, X. Z., Yu, J. H., Cai, Y. F. Contrib. Mineral. Petrol., 171(2016), 1–11, https://doi.org/10.1007/s00410-016-1252-x

[13] Li, Y., Jiang, H. T., Yang, X. Z. Geochim. Cosmochim. Ac., 217(2017), 16–27, https://doi.org/10.1016/j.gca.2017.08.020
[14] Huebner, J. S., Dillenburg, R. G. Am. Mineral., 80(1995), 46–64
[15] Manthilake, G., Mookherjee, M., Bolfan-Casanova, N., Andrault, D. Geophys. Res. Let., 42(2015), 7398–7405, https://doi.org/10.1002/2015GL064804
[16] Manthilake, G., Bolfan-Casanova, N., Novella, D., Mookherjee, M., Andrault, D. Sci. Adv., 2(2016), e1501631, https://doi.org/10.1126/sciadv.1501631
[17] Zhu, M. X., Xie, H. S., Guo, J., Bai. W. M., Xu, Z. M. Sci. China Earth Sci., 44(2001), 336–345, https://doi.org/10.1007/BF02907104
[18] Patro, P. K., Sarma, S. V. S., Naganjaneyulu, K. J. Geophys. Res. Solid Earth, 119(2014), 71–82, https://doi.org/10.1002/2013JB010430
[19] Xiao, Q. B., Zhang, J., Zhao, G. Z., Wang, J. J. Tectonophysics, 601(2013), 125–138, https://doi.org/10.1016/j.tecto.2013.05.003
[20] Wei, W. B., Jin, S., Ye, G. F., Deng, M., Jing, J. E., Unsworth, M., et al. *Sci. China Earth Sci*., 53(2009), 189–202, https://doi.org/10.1007/s11430-010-0001-7
[21] Xie, C. L., Jing, S., Wei, W. B., Ye, G. F., Zhang, L. T., Hao, D., et al. Earth Planets Space, 69(2017), 147, https://doi.org/10.1186/s40623-017-0734-z
[22] Wang, D. J., Mookherjee, M., Xu, Y. S., Karato, S. Nature, 443(2006), 977–980, https://doi.org/10.1038/nature05256
[23] Yang, X. Z., Keppler, H., McCammon, C., Ni, H. W., Xia, Q. K., Fan, Q. C. J. Geophys. Res., 116(2011), B04208, https://doi.org/10.1029/2010JB008010
[24] Sun, W. Q., Dai, L. D., Li, H. P., Hu, H. Y., Wu, L., Jiang, J. J. Am. Mineral., 102(2017a), 2450–2456, https://doi.org/10.2138/am-2017-6146
[25] Sun, W. Q., Dai, L. D., Li, H. P., Hu, H. Y., Jiang, J. J., Hui, K. S. Mineral. Petrol. 111(2017b), 853–863, https://doi.org/10.1007/s00710-017-0494-2
[26] Wang, D. J., Guo, X. Y., Yu, Y., Karato, S. Contrib. Mineral. Petr., 164(2012), 17–25, https://doi.org/10.1007/s00410-012-0722-z
[27] Wang, D. J., Liu, X. W., Liu, T., Shen, K. W., Welch, D. O., Li, B. S. Sci. Rep., 7(2017), 16893, https://doi.org/10.1038/s41598-017-16883-4
[28] Guo, X. Z., Yoshino, T., Shimojuku, A. Earth Planet. Sc. Lett., 412(2015), 1–9, https://doi.org/10.1016/j.epsl.2014.12.021
[29] Hashim, L., Gaillard, F., Champallier, R., Breton, N. L., Arbaret, L., Scaillet, B. Earth Planet. Sc. Lett., 373(2013), 20–30, https://doi.org/10.1016/j.epsl.2013.04.026
[30] Li, P., Guo, X. Z., Chen, S. B., Wang, C., Yang, J. L., Zhou, X. F. Contrib. Mineral. Petr., 173(2018), 16, https://doi.org/10.1007/s00410-018-1442-9
[31] Shimojuku, A., Yoshino, T., Yamazaki, D. Earth Planets Space, 66(2014), 1–9, https://doi.org/10.1186/1880-5981-66-2
[32] Sinmyo, R., Keppler, H. Contrib. Mineral. Petr., 172(2017), 4, https://doi.org/10.1007/s00410-016-1323-z
[33] Unsworth, M. J., Jones, A. G., Wei, W., Marquis, G., Gokarn, S. G., Spratt, J. E., Team, I. M. *Nature*, 438(2005), 78–81, https://doi.org/10.1038/nature04154
[34] Ferri, F., Gibert, B., Violay, M., Cesare, B. Tectonophysics, 586(2013), 84–94, https://doi.org/10.1016/j.tecto.2012.11.003
[35] Gaillard, F. J. Geophys. Res. Solid Earth, 110(2005), B06204, https://doi.org/10.1029/2004JB003282
[36] Gaillard, F., Malki, M., Iacono-Marziano, G., Pichavant, M., Scaillet, B. Science, 322(2008), 1363–1365, https://doi.org/10.1126/science.1164446
[37] Ghosh, D. B., Karki, B. B. Sci. Adv., 3(2017), e1701840, https://doi.org/10.1126/sciadv.1701840
[38] Laumonier, M., Gaillard, F., Sifre, D. Chem. Geol., 418(2015), 66–76, https://doi.org/10.1016/j.chemgeo.2014.09.019
[39] Laumonier, M., Gaillard, F., Muir, D., Blundy, J., Unsworth, M. Earth Planet. Sc. Lett., 457(2017), 173–180, https://doi.org/10.1016/j.epsl.2016.10.023
[40] Maumus, J., Bagdassarov, N., Schmeling, H. Geochim. Cosmochim. Ac., 69(2005), 4703–4718, https://doi.org/10.1016/j.gca.2005.05.010
[41] Wei, W. B., Unsworth, M., Jones, A. G., Booker, J., Tan, H, Nelson, K. D., et al. Science, 292(2001), 716–718, https://doi.org/10.1126/science.1010580
[42] Bagdassarov, N., Golabek, G. J., Solferion, G., Schmidt. M. W. Phys. Earth Planet. In., 177(2009), 139–146, https://doi.org/10.1016/j.pepi.2009.08.003

[43] Padilha, A. L., Vitorello, I., Antunes, C. E., Padua, M. B. J. Geophys. Res. Solid Earth, 120(2015), 4702–4719, https://doi.org/10.1002/2014JB011657
[44] Jones, A. G., Ledo, J., Ferguson, I. J. Can. J. Earth Sci., 42(2005), 457–478, https://doi.org/10.1139/E05-018
[45] Chen, J. Y., Yang, X. S., Chen, J. Y. J. Geophys., 60(2017), 3475–3492, https://doi.org/10.6038/cjg20170917
[46] Freund, F. J. Geodyn., 35(2003), 353–388, https://doi.org/10.1016/S0264-3707(02)00154-0
[47] Pous, J., Munoz, G., Heise, W., Melgarejo, J. C., Quesada, C. Earth Planet. Sc. Lett., 217(2004), 435–450, https://doi.org/10.1016/S0012-821X(03)00612-5
[48] Buseck, P. R., Beyssac, O. Elements, 10(2014), 421–426, https://doi.org/10.2113/gselements.10.6.421
[49] Luque, F. J., Pasteris, J. D., Wotapenka, B., Rodas, M., Barrenechea, J. F. Am. J. Sci., 298(1998), 471–498, https://doi.org/10.2475/ajs.298.6.471
[50] Luque, F. J., Huizenga, J. M., Crespo-Feo, E., Wada, H., Ortega, L., Barrenechea, J. F. Miner. Deposita, 49(2014), 261–277, https://doi.org/10.1007/s00126-013-0489-9
[51] Martín-Méndez, I., Boixereu, E., Villaseca, C. Miner. Deposita, 51(2016), 575–590, https://doi.org/10.1007/s00126-015-0625-9
[52] Gálvez, M. E., Beyssac, O., Martinez, I., Benzerara, K., Chaduteau, C., Malvoisin, B., et al. Nat. Geosci., 6(2013), 473–477, https://doi.org/10.1038/NGEO1827
[53] Kopylova, M. G., Beausoleil, Y., Goncharov, A., Burgess, J., Strand, P. Tectonophysics, 672(2016), 87–103, https://doi.org/10.1016/j.tecto.2016.01.034
[54] Spetsius, Z. V., Cliff, J., Griffin, W. L., O'Reilly, S. Y. Chem. Geol., 455(2017), 131–147, https://doi.org/10.1016/j.chemgeo.2016.11.002
[55] Pommier, A., Leinenweber, K., Tasaka, M. Earth Planet. Sc. Lett., 425(2015), 242–255, https://doi.org/10.1016/j.epsl.2015.05.052
[56] Roberts, J. J., Tyburczy, J. A. J. Geophys. Res. Solid Earth, 96(1991), 16205–16222, https://doi.org/10.1029/91JB01574
[57] Saltas, V., Chatzistamou, V., Pentari, D., Paris, E., Triantis, D., Fitilis, I., et al. Mater. Chem. Phys., 139(2013), 169–175, https://doi.org/10.1016/j.matchemphys.2013.01.016
[58] Wang, D. J., Karato, S., Jiang, Z. T. Geophys. Res. Let., 40(2013), 2028–2032, https://doi.org/10.1002/grl.50471
[59] Saltas, V., Vallianatos, F., Gidarakos, E. Appl. Clay Sci., 80–81(2013), 226–235, https://dx.doi.org/10.1016/j.clay.2013.02.028
[60] Yoshino, T., Matsuzaki, T., Shatzkiy, Y., Katsura, T. Earth Planet. Sc. Lett., 288(2009), 291–300, https://doi:10.1016/j.epsl.2009.09.032
[61] Wang, D. J., Li, H. P., Li, Y., Matsuzaki, T., Yoshino, T. J. Geophys. Res. Solid Earth, 115(2010), 633–650, https://doi.org/10.1029/2009JB006695
[62] Fuji-ta, K., Katsura, T., Tainosho, Y. Geophys. J. Int., 157(2004), 79–86, https://doi.org/10.1111/j.1365-246X.2004.02165.x
[63] Fuji-ta, K., Katsura, T., Matsuzaki, T., Ichiki, M., Kobayashi, T. Tectonophysics, 434(2007), 93–101, https://doi.org/10.1016/j.tecto.2007.02.004
[64] Baiju, K. R., Satish-Kumar, M., Kagi, H., Nambiar, C. G., Ravisankar, M. Gondwana Res., 8(2005), 223–230, https://doi.org/10.1016/S1342-937X(05)71120-5
[65] Huang, X. G., Xu, Y. S., Karato, S. Nature, 434(2005), 746–749, https://doi.org/10.1038/nature03426
[66] Xie, C. L., Jin, S., Wei, W. B., Ye, G. F., Jing, J. N., Zhang, L. T., et al. Tectonophysics. 675(2016), 168–180, https://doi.org/10.1016/j.tecto.2016.03.017
[67] Xie, C. L., Jing, S., Wei, W. B., Ye, G. F., Zhang, L. T., Hao, D., et al. Earth Planets Space, 69(2017), 147, https://doi.org/ 10.1186/s40623-017-0734-z
[68] Robertson, K., Taylor, D., Thiel, S., Heinson, G. Gondwana Res., 28(2015), 201–211, https://doi.org/ 10.1016/j.gr.2014.07.013
[69] Pommier, A., Leinenweber, K., Kohlstedt, D. L., Qi, C., Garbero, E. J., Mackwell, S. J., et al. Nature, 522(2015), 202–208, https://doi.org/10.1038/nature14502